Aluminum Substitution in Rutile Titanium Dioxide: New Constraints from High-Resolution ^{27}Al NMR

Jonathan F. Stebbins

Department of Geological and Environmental Sciences, Stanford University, Stanford, California 94305

Received December 7, 2006. Revised Manuscript Received January 26, 2007

The substitution of aluminum oxide into rutile (TiO_2) has major effects on crystal growth, cation diffusivity, and conductivity and, critical for its widespread application as a white pigment, inhibits photocatalytic activity. High-field, high-resolution ^{27}Al NMR provides unique constraints on the type and concentrations of several Al sites in rutile. For samples ranging from about 0.2 to 1 wt % Al_2O_3, annealed at 1000−1500 °C, Al in ordered, isolated octahedra (Ti sites) can be quantified. At the higher concentrations, Al in other disordered octahedral sites becomes predominant and may be due to both Ti sites with Al neighbors and to interstitials. The NMR line shape of this disordered component resembles that of Al_2TiO_5, for which new data are also presented. In all rutile samples, significant concentrations of Al in four-coordinated sites (and possibly in five-coordinated sites) are detected. In samples doped with equimolar Nb_2O_5, Al in isolated Ti sites is predominant at all concentrations. Temperature has only minor effects on relative concentrations of Al species, but strongly affects total solubility. In samples with excess or exsolved α-Al_2O_3 (corundum), solubility at 1200 °C is 0.56 ± 0.04 wt % and at 1000 °C is 0.23 ± 0.02 wt %.

Introduction

Titanium dioxide (TiO_2) is a well-known photosemiconductor and photocatalyst, which is of growing interest in a number of new technologies, including solar hydrogen production[1] and the UV-induced oxidation of organic compounds in wastewater.[2] However, for the high-temperature polymorph rutile, these same light-induced electronic properties must be mitigated for its major, long-standing application as a white pigment, to prevent degradation of polymer binders in paints and other coatings.[3,4] For this purpose, rutile is doped with small amounts of Al_2O_3 (typically <1 wt %). Al^{3+} dissolved in the bulk crystal plays an important part in reducing photoactivity, apparently by leading to the formation of oxygen vacancies that can trap charge carriers;[4] Al at crystallite surfaces also has a significant effect, which can in part be explained by reduced surface hydroxylation.[4] Al has large effects on crystal growth and transformation kinetics of both anatase and rutile,[5−8] on dopant cation diffusivities,[9] and on conductivity,[10] all of which are important in technological applications.

Rutile is also a common minor mineral in metamorphic and plutonic igneous rocks, where it invariably contains significant amounts of a number of three-, five-, and two-valent cations, sometimes reaching tens of percent.[11] The phase is isostructural with a high pressure form of SiO_2, stishovite (stable above about 10 GPa[12]), which has been found in impact craters and may occur in deeply subducted crustal rocks,[13] where trace Al substitution may be linked to hydrogen content and thus to water transport in the mantle.[14,15] Despite the technological and geochemical importance of such substitutions in rutile, understanding of solid solution mechanisms and energetics remains incomplete, in part because of the difficulty with uniquely characterizing the types and occupancies of low-abundance cations on various crystallographic and defect sites in the crystal.

In bulk rutile, several mechanisms for Al substitution have been proposed. Experimental and theoretical evidence for both have been reviewed in detail recently.[6,16] One possibility is a coupled reaction to replace Ti^{4+} with Al^{3+} on normal (substitutional) octahedral sites, compensating the lower cationic charge with oxygen vacancies

$$Al_2O_3 \rightleftharpoons 2Al_{Ti}' + V_O^{\bullet\bullet} + 3O_O \quad (1)$$

In this case, vacancies could be ordered with single or pairs of Al^{3+} cations, resulting in lowered Al coordination number,

(1) Nowotny, J.; Sorrell, C. C.; Bak, T.; Sheppard, L. R. *Sol. Energy* **2005**, *78*, 593.
(2) Bahnemann, D. *Sol. Energy* **2004**, *77*, 445.
(3) Gesenhues, U. *Chem. Eng. Technol.* **2001**, *24*, 685.
(4) Gesenhues, U. *J. Photochem. Photobiol., A* **2001**, *139*, 243.
(5) Gesenhues, U. *Sol. State Ionics* **1997**, *101−103*, 1171.
(6) Gesenhues, U.; Rentschler, T. *J. Solid State Chem.* **1999**, *143*, 210.
(7) Zhang, H.; Banfield, J. F. *Mater. Res. Bull.* **2000**, *15*, 437.
(8) Karvinen, S. *Solid State Sci.* **2003**, *5*, 811.
(9) Sasaki, J.; Peterson, N. L.; Hoshino, K. *J. Phys. Chem. Solids* **1985**, *46*, 1267.
(10) Bak, T.; Burg, T.; Kang, S.-J. L.; Nowotny, J.; Rekas, M.; Sheppard, L.; Sorrell, C. C.; Vance, E. R.; Yoshida, Y.; Yamawaki, M. *J. Phys. Chem. Solids* **2003**, *64*, 1089.
(11) Vlassopoulos, D.; Rossman, G. R.; Haggerty, S. E. *Am. Mineral.* **1993**.
(12) Panero, W. R.; Benedetti, L. R.; Jeanloz, R. *J. Geophys. Res.* **2003**, *108*, 2039.
(13) Ono, S.; Ohishi, Y.; Isshiki, M.; Watanuki, T. *J. Geophys. Res.* **2005**, *110*, B02208.
(14) Panero, W. R.; Stixrude, L. P. *Earth Planets Sci. Lett.* **2004**, *221*, 421.
(15) Pawley, A. R.; McMillan, P. F.; Holloway, J. R. *Science* **1993**, *261*, 1024.
(16) Steveson, M.; Bredow, T.; Gerson, A. R. *Phys. Chem. Chem. Phys.* **2002**, *4*, 358.

10.1021/cm0629053 CCC: $37.00
Published on Web 03/06/2007

or could be disordered throughout the crystal, lowering free energy by increasing configurational entropy. The latter might be expected, especially at high temperature.

A second type of mechanism maintains overall charge neutrality through the addition of extra Al^{3+} cations into normally unoccupied interstitial sites, which could be either octahedral or tetrahedral, as both occur in the structure

$$2Al_2O_3 \rightleftharpoons 3Al_{Ti}' + Al_i^{\bullet\bullet\bullet} + 6O_O \quad (2)$$

From observations of changes in IR spectra on addition of Al to rutile formed at temperatures of about 930−980 °C, it was suggested that mechanism 1 was most important at low alumina contents.[6] At relatively higher Al contents, the appearance of a shoulder on an IR band resembling a band in α-alumina (corundum) supported the growing importance of this second mechanism, suggesting the formation of face-shared pairs of Al-occupied octahedra in adjoining Ti sites and octahedral interstices.[6] In the same report, a change in predominant solution mechanism with composition was supported by X-ray diffraction, which indicated a decrease, followed by an increase, in O−O distances with increasing alumina content.[6]

A theoretical study using a classical force-field model suggested some energetic favorability to mechanism 1, but noted that mechanism 2 was not greatly less favorable, particularly if clustering of Al in Ti sites and in interstitials occurs.[17] A more recent study by semiempirical quantum chemical methods[16] explored a number of variations on both mechanisms, including association of vacancies and of Al and Ti interstitials with Al in Ti sites. All of the interstitial models were much less energetically stable than the substitutional models. However, the calculated energies of Al in isolated Ti sites with six oxygen neighbors, vs Al in adjacent Ti sites with a shared oxygen vacancy, were quite close, suggesting that both species could be present at low Al concentrations.[16]

The overall solubility of Al in rutile at relatively high temperatures has been determined from XRD measurements of the unit cell, which changes systematically with Al content until saturation is reached, and ranges from 0.6 wt % Al_2O_3 at 1200 to 2.0 wt % at 1426 °C.[18] These results, including the effects of co-addition of Nb^{5+}, were analyzed thermodynamically and found to support an interstitial model.[18] Studies of Al-doped, ultrafine rutile crystals, acid-etched to remove Al-rich surface layers, suggested, however, that the bulk solubility at 980 °C was much higher than the value predicted by extrapolation down in temperature from the previous data set (roughly 0.03 wt %).[5] The lower temperature solubilities are especially interesting because rutile for technological applications is often produced at temperatures near 1000 °C.[3]

As in other aliovalent solid solutions, coupled substitutions of charge-compensating cations have been explored in rutile. For example, equimolar substitution of tri- and pentavalent cations such as Al^{3+} and Nb^{5+} enhances solubility of both by eliminating the need for energetically unfavorable oxygen vacancies and cation interstitials[18]

$$Al_2O_3 + Nb_2O_5 \rightleftharpoons 2Al_{Ti}' + 2Nb_{Ti}^{\bullet} + 8O_O \quad (3)$$

At low oxygen pressures, contents of Ti^{3+} grow in rutile TiO_{2-x} and can be important in charge-compensating both tri- and pentavalent substituents, as well as in electronic and catalytic properties.[19] In both rutile and especially in isostructural stishovite, a charge-coupled substitution of H^+ and Al^{3+} may also be significant, at least in natural, water-rich environments; coupled substitutions of other metal oxides are of course common as well.[11,12,14,15,20]

Solid-state NMR has not been commonly applied to characterize sites occupied by minor constituents in inorganic crystals, as its sensitivity is generally much lower than that of other methods such as optical, IR, and X-ray spectroscopy. However, at high magnetic fields (e.g., 14.1 and 18.8 T, as described here), for nuclides with high natural abundance and high resonant frequencies such as ^{27}Al, quantitative, high-resolution spectra can often be readily obtained on even small (a few milligrams) samples containing only a fraction of a percent to a few percent of the element of interest. For example, recent studies of about 1 wt % Al_2O_3 in stishovite revealed Al in undistorted, octahedral sites only.[21] In an early magic-angle spinning (MAS) and single-crystal NMR study of Al in rutile, conducted at lower field (9.4 T), one type of site was clearly resolved and concluded to be Al in normal octahedral Ti sites, with no Al neighbors.[22] However, other broader spectral components, accounting for much of the total signal, were less readily characterized. In this study, we present high-field ^{27}Al MAS NMR data on a series of rutile samples equilibrated with Al_2O_3 contents of 0.2−0.9 wt % and annealed at temperatures from 1000 to 1500 °C. Results indicate a rich complexity to the distribution of Al in the crystals, confirm that both substitutional and interstitial mechanisms could be important depending on composition, and refine the solubility at relatively low temperatures.

Experimental Section

Sample Synthesis and Heat Treatment. Samples were prepared from finely powdered, high-purity TiO_2 (Sigma-Aldrich, 99.999%, particle size <1 μm) and reagent-grade $Al(OH)_3$ (MCB, gibbsite). The TiO_2 reagent was analyzed for Nb by ICP-AE; the element was not detected (<50 ppm). These were mixed in small quantities (<1 g) by successive dilution to obtain samples with 0.91, 0.46, and 0.18 wt % Al_2O_3 and then thoroughly ground in an agate mortar. A second set of samples was prepared with an alumina mortar to evaluate effects of silica contamination during grinding. TiO_2 samples with no added Al were run through the same grinding and heating procedures to test for reagent purity. All samples were packed into small Pt tubes and initially heated for 156 h at 1200

(17) Sayle, D. C.; Catlow, C. R. A.; Perrin, M. A.; Nortier, P. *J. Phys. Chem. Solids* **1995**, *56*, 799.
(18) Slepetys, R. A.; Vaughn, P. A. *J. Phys. Chem.* **1969**, *73*, 2157.
(19) Bak, T.; Nowotny, J.; Rekas, M.; Sorrell, C. C. *J. Phys. Chem. Solids* **2003**, *64*, 1057.
(20) Smyth, J. R.; Swope, R. J.; Pawley, A. R. *Am. Mineral.* **1995**, *80*, 454.
(21) Stebbins, J. F.; Du, L.-S.; Kelsey, K.; Kojitani, K.; Akaogi, M.; Ono, S. *Am. Mineral.* **2006**, *91*, 337.
(22) Stebbins, J. F.; Farnan, I.; Klabunde, U. *J. Am. Ceram. Soc.* **1989**, *11*, 2198.

°C in flowing O_2 gas to limit Ti^{3+} to insignificant concentrations,[19] ground again, and then heated a second time (182 h) at this temperature. Samples were quenched simply by removing them from the furnace: their small size (50−400 mg) led to cooling to room temperature within a few tens of seconds. This initial temperature was chosen to be well below that at which Al_2TiO_5 is stabilized (1240 °C[18]). Resulting crystallite sizes (roughly 10−20 μm) were large enough, and surface areas small enough, to make observation of surface Al species unlikely. Subsequently, portions of these samples were annealed for 114 h at 1422 °C or for 180 h at 1000 °C, again in O_2 gas. A portion of the 0.46 wt % alumina starting material was also doped with an equimolar amount of Nb_2O_5; this mixture was subjected to the same series of heat treatments as described above. Annealing conditions were similar to those used in a previous solubility study,[18] but run times used here were about five times longer.

In preliminary experiments, several other samples were synthesized from the same reagents with somewhat different thermal histories that nonetheless provide useful comparisons. One sample, with 0.2 wt % Al_2O_3, was heated in air at 1500 °C for 59 h with three intermediate grinding steps and used to compare NMR spectra from 14.1 and 18.8 T fields. A Al_2TiO_5 sample was described earlier;[22] powder X-ray diffraction data for a sample of γ-Al_2O_3 (Alfa-Aesar) and ^{27}Al MAS NMR at 14.1 T were nearly identical with previous reports on this material.[23,24]

NMR Experiments. ^{27}Al MAS NMR spectra were collected with Varian Unity/Inova spectrometers at 14.1 and 18.8 T fields, with Varian/Chemagnetics 3.2 mm "T3" probes and sample spinning rates of 20 kHz. Sample weights were typically 45−50 mg; a small rotor background signal from the stabilized ZrO_2 ceramic (estimated Al_2O_3 content about 32 ppm) was subtracted from all spectra. Frequencies are referenced to 0.1 M aqueous $Al(NO_3)_3$. Typical radiofrequency pulse powers of about 130 kHz and rf tip angles of about 30° (solid) were used. After preliminary studies of relaxation rates, it was concluded that short pulse delays (0.1 s) gave high-quality, nearly relaxed spectra for the broader components (typically 200 000−400 000 signal averages). However, the narrow component representing Al^{3+} in Ti octahedral sites (peak F, see Results) relaxed considerably more slowly, requiring a pulse delay of 1−5 s for full relaxation. Spectra of all samples were therefore also obtained with the latter delay (typically 5000−20000 signal averages). Pure samples of corundum, γ-alumina, and Al_2TiO_5[22] were also run as intensity standards and to directly compare observed peak shapes. About 8 μs of instrumental "dead time" was compensated by a linear back prediction algorithm in the processing of all data.

To determine the relative fractions of Al in the various components of the spectra, we determined peak areas by either subtraction of experimental (corundum) or simulated peak shapes (Al in Ti sites) and integration, or direct integration of specific regions of the spectrum (tetrahedral Al). Data from 14.1 and 18.8 T were compared to roughly estimate the relative effects of quadrupolar broadening and chemical shift disorder on the shapes of the broad components, but we did not attempt to completely fit complex disordered line shapes, as too many unconstrained parameters would be required given the obtained signal-to-noise ratios. The quadrupolar line shape for Al in Ti sites (see below) was fitted using the Varian "STARS" software.

(23) MacKenzie, K. J. D.; Temuujin, J.; Smith, M. E.; Angerer, P.; Kameshima, Y. *Thermochim. Acta* **2000**, *359*, 87.
(24) Wefers, K.; Misra, C. *Oxides and Hydroxides of Aluminum (Alcoa Technical Paper 19, Revised*); Alcoa Laboratories: Alcoa Center, PA, 1987.

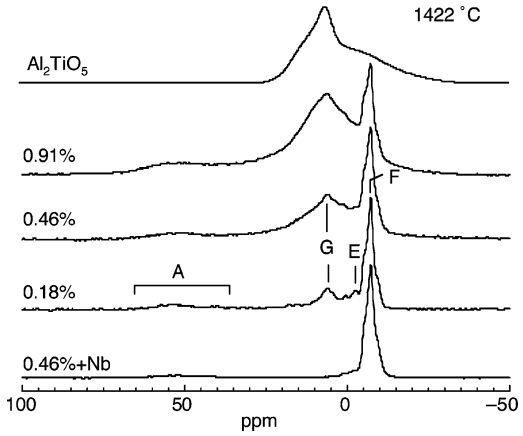

Figure 1. ^{27}Al MAS spectra for rutile samples with wt % Al_2O_3 as labeled, annealed at 1422 °C (Table 1), and for Al_2TiO_5. Spectra collected with a pulse delay of 0.1 s. Spinning sidebands are outside of the region displayed. Intensities are normalized to the highest peak in each spectrum. Assignments of labeled peaks are discussed in the text; label A shows region for [4]Al, other peaks are for various types of [6]Al.

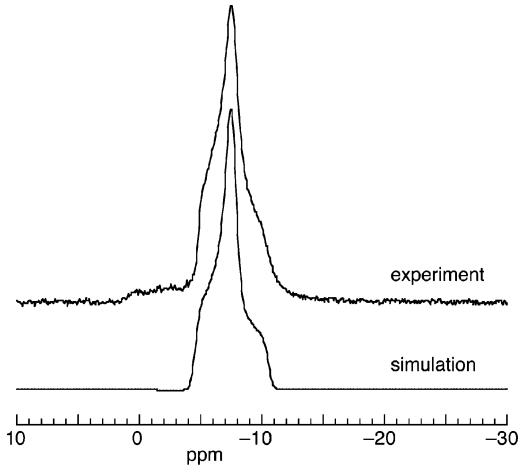

Figure 2. ^{27}Al MAS spectra for rutile sample with 0.46 wt % Al_2O_3 and co-doped with Nb_2O_5, annealed at 1200 °C, compared with simulated quadrupolar line shape ($C_Q = 2.9 \pm 0.05$ MHz; $\eta = 1.0$; $\delta_{iso} = -5 \pm 0.5$ ppm).

Results

Components of Spectra. Spectra of undoped rutile showed no ^{27}Al NMR signal above background (<0.01 wt % Al_2O_3.) Spectra for all of the Al-doped rutile samples were complex and each contained between two and five partially resolved components. We begin by describing results for samples annealed at 1422 °C (Figure 1). Appearing in all spectra, and predominant in data for samples with the lowest Al concentrations and in the Nb-doped samples is a sharp, narrow quadrupolar line shape (labeled F, peak maximum = −7.4 ppm) that can be readily fitted with $C_Q = 2.9 \pm 0.05$ MHz, quadrupolar asymmetry parameter $\eta = 1.0$, and isotropic chemical shift $\delta_{iso} = -5.0 \pm 0.5$ (Figure 2). This peak is the same as that described in our previous NMR study,[22] but is more accurately determined at the higher fields used here. It showed a significantly slower spin−lattice relaxation rate than the broader components of the spectra, as illustrated by a comparison of relative peak intensities for pulse delays of 0.1 and 5 s (Figure 3). As discussed below, this peak is readily assigned as Al in simple, isolated Ti sites.

Other peaks are also seen in the typical range for [6]Al (roughly 15 to −10 ppm). At 0.18%, this is represented

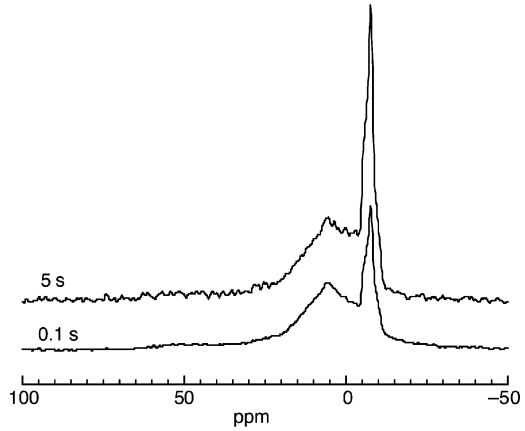

Figure 3. ^{27}Al MAS spectra for rutile sample with 0.46 wt % Al_2O_3, annealed at 1200 °C, showing differences in relative intensities for data collected with pulse delays of 0.1 vs 5 s. Spectra are plotted with the same absolute intensity, scaled by the number of signal averages.

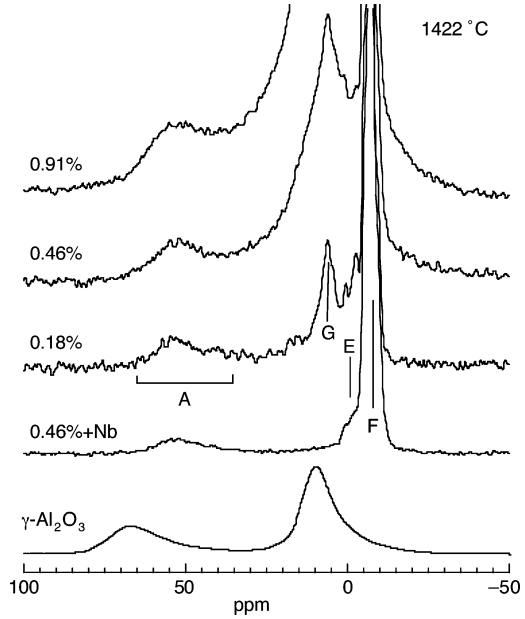

Figure 4. ^{27}Al MAS spectra for rutile samples with wt % Al_2O_3 as labeled, annealed at 1422 °C (Table 1), and for γ-Al_2O_3. Spectra are the same as those in Figure 1, with vertical scales enlarged by 500%. Intensities are normalized to the highest peak in each spectrum, except for γ-Al_2O_3.

primarily by a relatively narrow peak (G) centered at 6 ppm and a smaller, narrow peak (or peaks?) at +0.5 to −3 ppm (E); as Al concentration grows, these components broaden considerably, merge, and begin to resemble the spectrum of Al_2TiO_5 (Figure 1).

In all spectra, another broad component is observed, centered at about 52 ppm (component A, Figure 4), which can be attributed to tetrahedral Al ($^{[4]}$Al).[25] Data for several samples from 18.8 T, when compared to those collected at 14.1 T, indicates relatively minor effects of field on peak width and position of this component as well as the broad $^{[6]}$Al component (Figure 5). Their widths thus have large contributions from distributions of chemical shift (and possibly C_Q), indicating considerable local disorder. The position of the A peak cannot be due to the presence of γ-Al_2O_3 or other "transition" aluminas, as it is about 15 ppm

(25) MacKenzie, K. J. D.; Smith, M. E. *Multinuclear Solid-State NMR of Inorganic Materials*; Pergamon: New York, 2002.

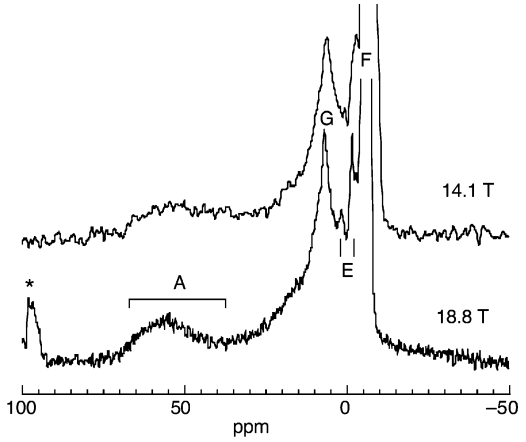

Figure 5. ^{27}Al MAS spectra for the rutile sample with 0.2 wt % Al_2O_3, annealed in air at 1500 °C, collected at 14.1 and 18.8 T with a 0.1 s pulse delay. A spinning sideband in the latter is marked by an asterisk. Intensities are normalized to the highest peak in each spectrum, enlarged by about 10×.

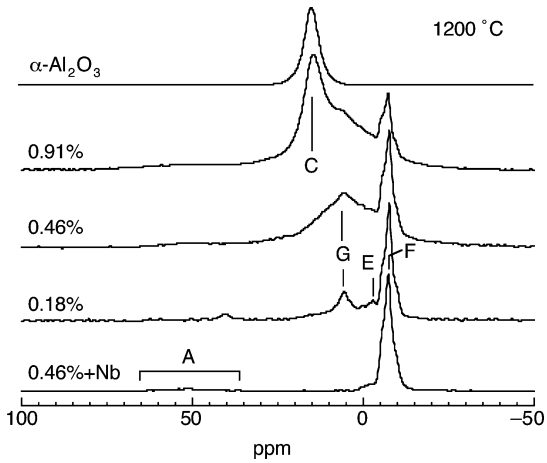

Figure 6. ^{27}Al MAS spectra for rutile samples with wt % Al_2O_3 as labeled, annealed at 1200 °C (Table 1), and for α-Al_2O_3 (corundum, marked C). Spectra collected with a pulse delay of 0.1 s. Intensities are normalized to the highest peak in each spectrum.

below typical $^{[4]}$Al peak positions for such phases (Figure 4). In any case, transition aluminas convert rapidly to corundum under these experimental conditions and are thus not expected in these samples. The possibility of the formation of mullite ($\approx Al_6Si_2O_{13}$, containing both $^{[4]}$Al and $^{[6]}$Al) from silica contamination during grinding was ruled out by the presence of similar A peaks in duplicate samples ground in an alumina mortar. Especially in samples with the most prominent A component (e.g., 0.91% alumina, 1422 °C), an additional broad, unresolved component is evident between about 40 and 25 ppm (Figure 4), the range typical for five-coordinated Al ($^{[5]}$Al).[25] This intensity is well above the high-frequency tail of even a highly disordered $^{[6]}$Al phase (e.g., Al_2TiO_5), but accurately quantifying this species is problematical.

In the spectrum for the 1200 °C sample with 0.91 wt % Al_2O_3 (Figure 6), another prominent, relatively narrow $^{[6]}$Al peak (C) is present whose shape and position (14.7 ppm) match those of corundum, indicating that this alumina content exceeded the solubility at this temperature. This component disappeared when the sample was heated to 1400 °C (Figure 1), as the corundum either dissolved in the rutile or reacted to form Al_2TiO_5, the stable phase for excess Al above 1240

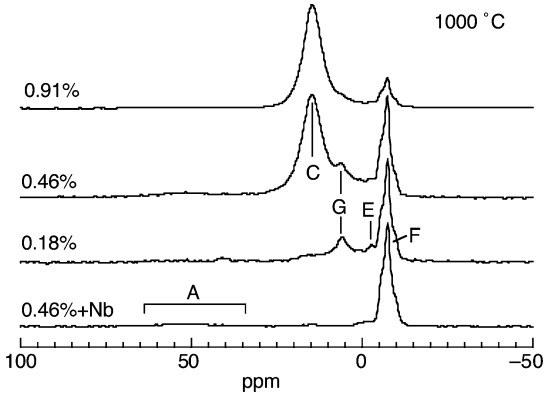

Figure 7. ^{27}Al MAS spectra for rutile samples with wt % Al_2O_3 as labeled, annealed at 1000 °C (Table 1). Spectra collected with a pulse delay of 0.1 s. Intensities are normalized to the highest peak in each spectrum.

°C.[18] The 0.46 wt % sample synthesized at 1200 °C contained little or no detectable corundum but, when annealed at 1000 °C, exsolved corundum and developed a prominent C peak (Figure 7), as did the 0.91% sample.

Effects of Al Concentration and Nb on Al Site Distribution. Fully relaxed spectra collected with pulse delays of 5 s were analyzed to determine the relative proportions of various components. For the three samples containing corundum, a slightly broadened experimental line shape for this material was subtracted and the change in the total integral determined; this allowed the saturation level of alumina to be determined. For all spectra, $^{[4]}$Al content was estimated simply by integration from 80 to 25 ppm; this region may contain the signal for some unresolved $^{[5]}$Al as well. A simulated quadrupolar line shape for the F peak was also subtracted, to allow estimation of the residual broad $^{[6]}$Al (G) component. Results are given in Table 1, which also shows the total dissolved (non-corundum) alumina contents, and in Figure 8. In unsaturated samples, all three dissolved components (B, G, F) increase with total alumina, but the broad $^{[6]}$Al component (G) increases much more rapidly and predominates at the higher concentrations. For the samples saturated with corundum, parts b and c of Figure 8 plot component fractions both at the total alumina content and at the estimated dissolved content. For the samples annealed at 1000 °C, dissolved component fractions estimated for both samples containing corundum (0.46 and 0.91% total alumina) are in good agreement. For all three temperatures, the 0.46% alumina samples co-doped with Nb_2O_5 contain a much higher fraction of the F peak than do the Nb-free samples; on annealing at 1000 °C, this sample shows no sign of corundum exsolution, indicating an alumina solubility at least twice that of the Nb-free sample.

To test the overall quantitation of the spectra, we compared integrated total peak areas (100 to −40 ppm) with those expected from nominal total alumina contents, sample weights, and data for samples of pure corundum and Al_2TiO_5. For the samples dominated by the narrow F peak (i.e., the Nb-doped samples), agreement was generally within about 5% of the expected value. For those with large broad components, total areas were generally about 10−20% low, probably because of a minor unintegrated component of the central transition in the first spinning sidebands and/or the loss of part of the low-frequency tail of the spectra in the noise of the baseline, problems accentuated by the low total signal and long relaxation times of these types of samples. Detailed simulations of the spinning sideband manifolds were not allowed by the overall signal-to-noise ratios of the fully relaxed spectra.

Effects of Temperature. The largest effect of temperature is on the overall solubility of alumina and a corresponding change with composition of the relative proportions of dissolved Al species at saturation (Figure 8). For a given dissolved alumina content, there seems to be some trend with increasing temperature for the fraction of $^{[4]}$Al (peak A), although data for these broad peaks are imprecise. For the samples in which most of the Al is in the F peak (0.18% alumina and Nb-doped samples), direct overlays of the spectra show negligible temperature effects on the relative proportions of the F component and the broader $^{[6]}$Al component. For the 0.46% samples annealed at 1200 and 1422 °C, though, which have a much higher proportion of the latter component, there is a minor increase in the proportion of the F component at higher temperature. Estimates of the fraction of the broad $^{[6]}$Al component in the samples containing corundum are relatively imprecise because of peak overlap and thus not very useful for assessing this aspect of temperature effects.

Discussion

Peak Assignments. As in our previous NMR study of Al in rutile,[22] the narrow F peak can readily be assigned to isolated Al in normal octahedral Ti sites. Its extremely negative chemical shift (one of the lowest observed for Al in a non-phosphate oxide) is consistent with Ti^{4+} instead of Al^{3+} neighbors by analogy to the effects of Si^{4+} vs Al^{3+} neighbors in chemical shifts in framework aluminosilicates;[25] a low chemical shift is also expected from the average M−O bond length in such sites (0.1958 nm[26]), as these are significantly longer than is typical for $^{[6]}$Al (e.g., 0.1914 nm in corundum[26]). Its well-defined line shape requires a high degree of local ordering, i.e., all Ti^{4+} neighbors and no adjacent vacancies or interstitial cations that would cause variations in chemical shift and quadrupolar parameters. Its relatively long spin−lattice relaxation time suggests a lack of coupling to nearby nuclear spins with high gyromagnetic ratios (^{27}Al and ^{93}Nb being the only candidates) or to electronic spins (e.g., Ti^{3+}). In our previous study,[22] the extreme narrowness of the corresponding single-crystal ^{27}Al NMR peaks also indicated a lack of homonuclear dipolar coupling to Al neighbors.

The position and shape of the F peak are identical in the samples doped only with Al_2O_3 and those doped with equimolar Nb_2O_5. This strongly suggests that whatever the mechanism of overall charge balance (oxygen vacancies, Al or Ti interstitials, Nb^{5+} cations), local charge balance is not maintained primarily by local pairing of a charge compensator with the Al^{3+} in Ti^{4+} sites. The ensuing distortion of the octahedron and effects on the ^{27}Al chemical shift and quadrupolar parameters would surely be different in the Nb-

(26) Smyth, J. R.; Bish, D. L. *Crystal Structures and Cation Sites of the Rock-Forming Minerals*; Allen and Unwin: Boston, 1988.

Table 1. Synthesis Conditions and Aluminum Speciation for Al-Doped Rutile[a]

name and temperature (± 5 °C)	total wt % Al_2O_3 (± 0.005)	dissolved wt % Al_2O_3	$^{[4]}Al$[b]	Al in Ti site (peak F)	Al in other dissolved $^{[6]}Al$
TA0.2S-1000	0.18	0.18(1)	0.017(4)	0.13(2)	0.13(2)
TA0.5S-1000	0.46	0.24(2)[c]	0.04(1)	0.21(2)	0.12(2)
TA1S-1000	0.91	0.21(2)[c]	0.02(1)	0.19(2)	0.12(2)
TA0.5S-Nb-1000[d]	0.46	0.46(1)	0.05(1)	0.56(5)	0.11(2)
TA0.2S-1200	0.18	0.18(1)	0.017(4)	0.14(2)	0.13(2)
TA0.5S-1200	0.46	0.46(1)	0.07(2)	0.20(2)	0.45(5)
TA1S-1200	0.91	0.56(4)[c]	0.10(3)	0.21(2)	0.56(5)
TA0.5S-Nb-1200[d]	0.46	0.46(1)	0.019(5)	0.56(5)	0.14(2)
TA0.2S-1422	0.18	0.18(1)	0.03(1)	0.15(2)	0.10(2)
TA0.5S-1422	0.46	0.46(1)	0.07(2)	0.22(2)	0.43(4)
TA1S-1422	0.91	0.91(1)	0.18(4)	0.26(3)	0.98(9)
TA0.5S-Nb-1422[d]	0.46	0.46(1)	0.03(1)	0.52(5)	0.16(2)

[a] All heat treatments were done in 1 bar O_2 except for that of TA0.2A-1500 (Figure 5), which was annealed in air (see text for details). Speciation data are in percent of total cations (Ti + Al + Nb). Unless otherwise noted, estimated uncertainties in the last decimalplace are given in parentheses. [b] May include some $^{[5]}Al$. [c] Remainder in excess or exsolved corundum. [d] Contains equimolar Al and Nb.

free vs Nb-doped samples if such pairing was predominant. In particular, if oxygen vacancies were present and paired with $^{[6]}Al$, the lowered coordination number and relaxation to shorter Al−O bond distances[16] would be expected to cause a significant increase in chemical shift toward values more typical for $^{[5]}Al$ (roughly 35 ppm[25]). Instead, it seems that at low Al concentrations, and in the Nb-doped samples, most of the charge compensators are distributed throughout the lattice by entropic effects of the high synthesis temperature.

The initially narrow peak G (e.g., in the 0.18% alumina samples) has a higher chemical shift than the F peak and is likely to represent Al either in octahedral interstices with slightly shorter mean distances, or Al in Ti sites that are in isolated pairs with other Al^{3+} cations (i.e., all other neighbors are Ti). At higher alumina contents, the relative and absolute proportions of these kinds of sites grow rapidly and the peak width increases, indicating considerable local disorder. The latter probably reflects a disordered distribution of Al and Ti neighbors in small clusters of Al in Ti and/or in interstitial sites, resulting in ranges of bond distances and causing ranges in chemical shifts and quadrupolar parameters. Clustering has been suggested from a variety of evidence, such as changes in IR spectra with alumina content[6] and modeling of energetics.[16] At the higher alumina contents, this feature resembles the spectrum of Al_2TiO_5, the structure of which is comprised of two types of edge-shared octahedral sites with disordered Al and Ti cations and which thus must contain many Al−Al octahedral pairs.[27,28] In this pseudobrookite-type structure, an unusual arrangement of chains of trioctahedral units has been noted.[27]

All of the samples studied here also contain minor amounts of Al (about 2 to >10% total Al) in tetrahedral sites, which is unexpected from most previous studies. Given the low surface areas (crystal sizes typically at least 10−20 μm), the observed $^{[4]}Al$ cannot be in surface defects. It could result from the association of two oxygen vacancies with Al in nominally octahedral sites, or with the entry of increasing Al^{3+} into tetrahedral interstices at higher temperature, which would be face-shared with octahedra containing either Al^{3+} or Ti^{4+}. Theoretical models suggest that structural relaxation around such defects may, however, blur the distinction between nominally octahedrally and nominally tetrahedral interstices.[16] It is also conceivable that with some local structural rearrangement, small, spinel-like clusters could form, with corner-shared tetrahedra and octahedra, increasing the cation−cation distances in such pairs and decreasing repulsive energy. In comparison with γ-alumina, which has a disordered spinel structure,[29] the observed $^{[4]}Al$ peaks in rutile are shifted down in frequency by about 15 ppm, suggesting unusually long mean Al−O distances and/or some Ti neighbors. As above, we note that, especially in the samples with highest alumina contents made at 1422 °C, there is significant unresolved intensity in the region where a signal from $^{[5]}Al$ is expected (roughly 40−25 ppm), whose intensity could be at least as great as that estimated for $^{[4]}Al$. Again, some vacancy or high-energy defect structure is implied.

Constraints on Solubility. Our estimate of alumina solubility at 1200 °C of 0.56 ± 0.04 wt % is in good agreement with the previous study of Slepetys and Vaughn,[18] who reported a value of 0.62 ± 0.1 wt % at this temperature for samples annealed in O_2 for 48 h after initial synthesis at higher temperature. The apparent dissolution of all excess alumina in our 0.91 wt % sample at 1422 °C is consistent with their solubility of 2.0%,[18] but NMR would not be able to clearly distinguish the presence of some Al_2TiO_5 in this sample because of the similarity of its peak shape to that of the broad, dissolved $^{[6]}Al$ component (Figure 1). Slepetys and Vaughn[18] proposed a marked steepening of the temperature slope to the alumina solubility below 1240 °C, where the stable aluminous phase changes from Al_2TiO_5 to corundum. The lower temperature slope was extrapolated to 980 °C to suggest a solubility of about 0.03 wt %, far below that estimated from samples in which surface alumina was removed by acid leaching (about 0.5 wt %)[5] and far below that estimated here from NMR spectra (0.23 wt %). Although some difference in slope is indeed to be expected with a different phase to buffer alumina activity, the large change suggested previously[18] may be unwarranted, given reported uncertainties. In Figure 9, the Slepetys and Vaughn data are plotted together with their estimates of standard deviations. A linear fit that is consistent with all of their results (log of

(27) Morosin, B.; Lynch, R. W. *Acta Crystallogr., Sect. B* **1972**, *28*, 1040.
(28) Norberg, S. T.; Ishizawa, N.; Hoffmann, S.; Yoshimura, M. *Acta Crystallogr., Sect. E* **2005**, *61*, 1160.
(29) Zhou, R. S.; Snyder, R. L. *Acta Crystallogr., Sect. B* **1991**, *67*, 617.

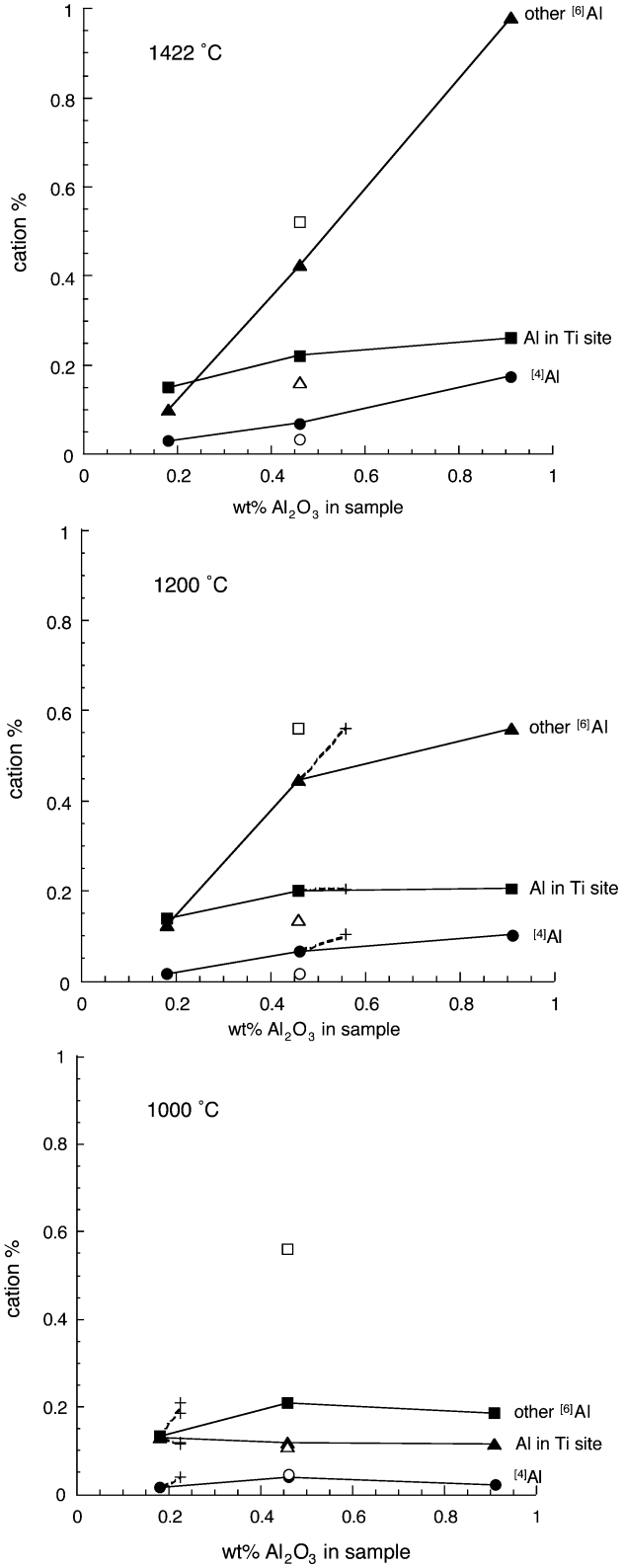

Figure 8. Fractions of dissolved Al components in rutile, in cation %, vs total wt % alumina in sample. Circles: $^{[4]}$Al (+ $^{[5]}$Al?); squares, Al in Ti sites (peak F); triangles, Al in other dissolved $^{[6]}$Al sites. Solid symbols denote samples doped with Al_2O_3 only; open symbols show data for samples doped with equimolar Al_2O_3 and Nb_2O_5. Note that the relative proportions of the $^{[6]}$Al components in the latter are reversed from the former. In the case in which some samples were saturated with corundum (b, c), points are also plotted at the measured saturation value of total alumina (dashed lines and + symbols).

solubility vs inverse temperature) extrapolates very close to the NMR datum at 1000 °C.

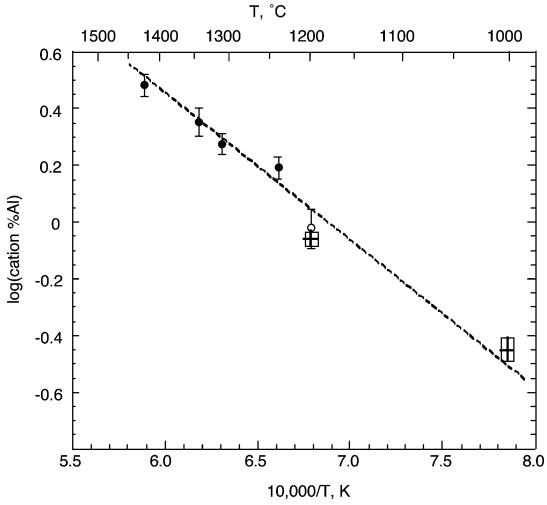

Figure 9. Logarithm of total dissolved Al, in cation %, vs inverse temperature. Circles show results of XRD data of Slepetys and Vaughn:[18] solid symbols denote rutile equilibrated with Al_2TiO_5, open symbol shows rutile equilibrated with α-Al_2O_3. Error bars are as originally published.[18] Dashed line is a fit to all of the XRD results. Boxed crosses show estimates based on NMR data for rutile with excess α-Al_2O_3.

Mechanisms of Solution. The structurally simplest solution mechanism for alumina in rutile, not surprisingly, is the charge-compensated substitution of equimolar amounts of Al^{3+} and Nb^{5+}. In such samples, most Al (typically 75% or more) occupies Ti octahedra, with only minor other $^{[6]}$Al and $^{[4]}$Al. As has long been appreciated,[18] this mechanism obviates the need for energetically costly interstitial cations and/or oxygen vacancies and can greatly enhance overall alumina (and niobia) solubility. The NMR data suggest as well that at least at 1000−1422 °C, there is not systematic local pairing of the trivalent and pentavalent cations.

^{27}Al NMR cannot directly determine the presence or absence of oxygen vacancies. It is clear that at low Al concentrations in Nb-free samples, the most abundant species is again Al in Ti octahedra with six oxygen neighbors, thus unpaired with vacancies if the latter are present. However, in all of the Nb-free samples, even at 0.18 wt % alumina, there are sufficient concentrations of "other" $^{[6]}$Al sites (G and/or E peaks) and/or $^{[4]}$Al sites for overall charge balance to occur if these are indeed interstitials, as only one interstitial per three Ti site substitutions would be required (eq 2). At the lowest concentrations, it is again clear that such interstitials are not locally paired with most of the Al in Ti sites. The presence of such other $^{[6]}$Al sites does not, on the other hand, rule out a vacancy mechanism at low concentrations. The transition at higher alumina contents to a mechanism in which most Al cations are in octahedra with Al neighbors, possibly due to significant interstitial occupancy, is consistent with recent conclusions from IR spectroscopy and XRD of a concentration-dependent mechanism.[6] The leveling off of the concentration of Al in isolated Ti sites with increasing total Al content (Figure 8a) may also suggest that the mechanism producing such sites is distinct from the one that dominates at high concentrations. Local structural rearrangement to Al_2TiO_5-like clusters of edge-shared Al and Ti octahedra is also a possibility suggested by the broad $^{[6]}$Al line shape and position at the higher alumina contents.

Most models of alumina solubility in rutile assume that Al is in octahedral sites, possibly with reduced coordination due to an associated oxygen vacancy. The NMR results support the predominance of $^{[6]}$Al, but show as well that $^{[4]}$Al and possibly $^{[5]}$Al can also be significant, up to at least 12% of the total in the highest temperature, highest concentration samples. Although this finding adds to the complexity of the problem, tetrahedral site occupancy has also been indicated by the finding, from ^{29}Si NMR, of only $^{[4]}$Si in silica-saturated rutile.[30,31]

Comparison with Stishovite. In samples of stishovite synthesized at 12−13 GPa and 1450−1600 °C in the presence of excess Al_2O_3 and H_2O, about 1 wt % alumina was found to be dissolved by high-field ^{27}Al MAS NMR.[21] The spectra showed a single, narrow peak with C_Q and η values (3.4 ± 0.4 MHz, 0.8 ± 0.2) similar to those reported here for the F peak in rutile. The isotropic chemical shift of 11 ppm is much higher, however, probably due to considerably shorter octahedral bond distances (mean Si−O distance of 0.1755 nm vs 0.1955 in rutile[26]). As for the isolated Al in Ti octahedra in rutile, it was concluded that oxygen vacancies, if present, were not paired with the Al-occupied octahedra in stishovite.[21] However, unlike rutile (especially at such a high alumina content), there is no evidence for other Al sites in the stishovite, indicating that solution mechanisms involving interstitial Al^{3+} or cation pairing are probably unimportant. This difference may arise from the correspondingly smaller size of the interstitial sites in stishovite compared to those in rutile: the volume of the occupied octahedron of the former, for example, is 34% less.[26] Although the content of hydrogen (OH) in the aluminous stishovite was not measured for the ^{27}Al NMR samples, their synthesis under H_2O-excess conditions suggested that at least part of the charge compensation for the Al^{3+} substitution was likely to be H^+, a mechanism that has been well-studied because of its possible importance in the transport of water into the Earth's mantle.[12,15] Although H^+ substitution can be an important mechanism of charge compensation in rutiles that grow in hydrous natural environments,[11,20] it is unlikely to be of much importance for rutile synthesized at high temperature and ambient pressure in dry gases.

We note finally an interesting parallel to a previous ^{27}Al NMR study[32] of a sample of the cement phase "belite" (Ca_2SiO_4) containing only 0.7 wt % Al_2O_3. $^{[4]}$Al substituting for Si was reported to have what may be the highest known chemical shift for this nuclide in an oxide, of 96 ppm. As mentioned above for $^{[6]}$Al in stishovite (and in a sense opposite to our description of the F site in rutile), this extreme value was attributed to the unusually short bond distances expected for Al in an Si site.

Conclusions

High-resolution ^{27}Al NMR can detect and quantify several distinct types of Al sites in alumina-doped rutile, down to concentrations well below 0.2 wt % Al_2O_3. Excess or exsolved corundum can readily be detected at abundances down to at least 0.05%. At low total alumina concentrations and in samples co-doped with equimolar Nb_2O_5, the predominant site is Al in isolated, symmetrical Ti octahedra, unpaired with vacancies or with Al^{3+} (or Nb^{5+}) in adjacent Ti sites or in interstitial sites, although lesser concentrations of other octahedral Al are present in all samples. At higher concentrations, other distinct octahedral Al sites become more important and probably represent Al in Ti octahedra with disordered Al neighbors and/or Al in octahedral interstices. A change in the predominant solubility mechanism with increasing Al content from one with overall charge balance for Al^{3+} in Ti^{4+} sites by oxygen vacancies to one with Al^{3+} interstitials[6] is consistent with these findings. Minor, but ubiquitous, concentrations of four-coordinated (and possibly five-coordinated) Al also develop, most obviously at higher total Al concentrations. Temperature affects total solubility, but does not greatly change relative proportions of Al species at a given total dissolved alumina level. Solubility at 1000 °C is much higher (about 0.23 wt % Al_2O_3) than predicted from previous studies of samples annealed at 1200 to 1426 °C[18] and closer to that estimated near 1000 °C from analysis of acid-etched samples.[5]

Acknowledgment. This study was funded by the U.S. National Science Foundation, Grant EAR 0408410. The author is grateful to J. Puglisi and C. Liu for access to the 18.8 T spectrometer at the Stanford Magnetic Resonance Laboratory, U. Gesenhues for numerous enlightening discussions of Al in rutile and comments on an early version of this paper, Guanchao Li for the ICP analysis, and two anonymous reviewers.

CM0629053

(30) Okada, K.; Yamamoto, N.; Kameshima, Y.; Yasumori, A.; MacKenzie, K. J. D. *J. Am. Ceram. Soc.* **2001**, *84*, 1591.
(31) Stebbins, J. F. *MRS Bull.* **1992**, *17*, 45.
(32) Skibsted, J.; Jakobsen, H. J.; Hall, C. *J. Chem. Soc., Faraday Trans.* **1994**, *90*, 2095.